VISUALIZATION OF A HYPERBOLIC STRUCTURE IN AREA PRESERVING MAPS

A.Giorgilli[1], V.F.Lazutkin[2], C.Simó[3]

[1] Università degli Studi di Milano,
[2] St.-Petersburg State University,
[3] Universitat de Barcelona

Abstract. We present a simple method which displays a hyperbolic structure in the phase space of an area preserving map. The method is illustrated for the case of the Carleson standard map. As it follows from our experiments, the structure of the chaotic zone for the standard map is different from the one found for the systems of Anosov type.

§1. Introduction.

One of the most misterious and, probably, difficult problems in modern dynamics is that of the *coexistence of regular and chaotic motions* in Hamiltonian dynamical systems [S]. If the number of degrees of freedom exceeds 1, both types of motions appear in the phase space of most of known examples, such as the standard map, the double pendulum, the three body problem, etc. The famous KAM theory gives us plenty of information concerning the regular part of the motion whilst almost nothing is known about the structure of the chaotic part. In the case of area preserving maps the regular part is represented by invariant circles, or periodic chains of invariant circles. The latter form structures which are often referred to as *islands.* There are also gaps between circles and the motion on them displays some kind of chaos. Apparent regions filled by chaotic trajectories are called *stochastic layers.* To the best of our knowledge, it was Hénon who discovered such regions (see [HH] and also [H] for historical comments). Of course, Poincaré knew the extremely intricated character of the motion [Po]. To illustrate the above description of the coexistence of different kinds of motion, we present here a picture of the phase portrait of the map

$$\begin{pmatrix} x \\ y \end{pmatrix} \mapsto \begin{pmatrix} 0.2\cos 2\pi x - y \\ x \end{pmatrix} \tag{1.1}$$

defined on the 2–torus $\mathbb{T}^2 = \mathbb{R}^2/\mathbb{Z}^2$. Only one quarter of the torus, namely the domain $|x| \le 1/4$, $|y| \le 1/4$, is drawn. The remaining part can be restored by symmetry (see [LS]).

One can see a big chaotic zone bounded by invariant circles of different types. The chaotic zone also contains islands (see [ST1,ST2]), and the regular part contains a

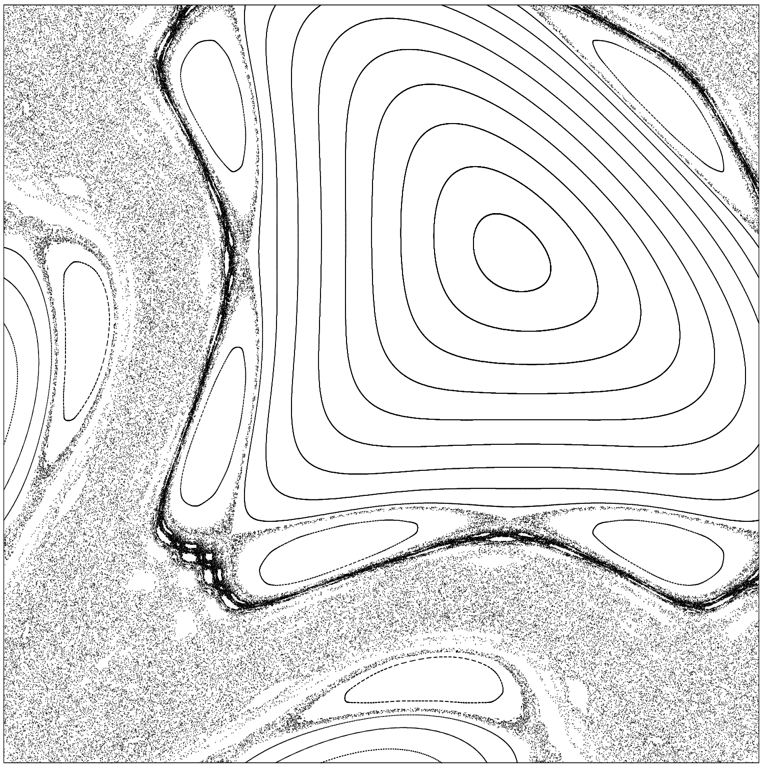

Figure 1. Several trajectories representing the characteristic features of the map (1.1) are drawn on one quarter of the torus, defined by the inequalities $-0.25 \le x \le 0.25$, $-0.25 \le y \le 0.25$.

lot of other thin chaotic zones in the resonant gaps between the KAM curves. They are invisible on the scale of Fig.1, but the common belief, supported by numerical evidence [BCGGS], is that they exist. In this context see also [Z].

As we have already mentioned, almost nothing is known, up to now, about the structure of the chaotic zone. The natural conjecture is the following one: *the chaotic zone is an invariant subset of positive Lebesgue measure, such that the restriction of the map onto it is isomorphic (in the sense of measure theory) to the product of a finite permutation and a Bernoulli shift.*

In order to prove this conjecture, one can apply Pesin's theory [Pes1,Pes2]. The starting point of Pesin's theory is the presence of a *hyperbolic structure.* Let us give the definition of a hyperbolic structure in the simplest case, that of area preserving maps. Let $F\colon S \to S$ be a smooth area preserving self–map of a surface S. Suppose that S is supplied with a Riemannian metric. We say that an invariant set $\Omega \subset S$ is *hyperbolic* if at each point $p \in \Omega$ there are two independent tangent vectors, $\vec{e}^{\,s}_p$, $\vec{e}^{\,u}_p$, such that the fields $p \mapsto \vec{e}^{\,s,u}_p$ are invariant, i.e.,

$$\begin{aligned} F'(p)\vec{e}^{\,s}_p &= C^s_p \vec{e}^{\,s}_{F(p)}\,, \\ F'(p)\vec{e}^{\,u}_p &= C^u_p \vec{e}^{\,u}_{F(p)}\,, \end{aligned}$$

and

$$
\begin{aligned}
&\lim_{n\to\pm\infty}\frac{1}{n}\log\|(F^n)'(p)\vec{e}_p^{\,s}\| = -\chi(p) < 0\,,\\
&\lim_{n\to\pm\infty}\frac{1}{n}\log\|(F^n)'(p)\vec{e}_p^{\,u}\| = \chi(p) > 0\,.
\end{aligned}
\tag{1.2}
$$

Here $F'(p)\colon T_pS \to T_pS$ is the *tangent* map to F at the point p, C_p^u and C_p^s stand for some nonzero constants, and the notation F^n is used to denote the n–th iterate of F, that is $F^n = \underbrace{F\circ F\circ\cdots\circ F}_{n\ \text{times}}$ for n positive and $F^n = \underbrace{F^{-1}\circ F^{-1}\circ\cdots\circ F^{-1}}_{-n\ \text{times}}$ for n negative integer.

The quantity $\chi(p)$ is called the *Lyapunov exponent* at a point p.

The fields of vectors $\{\vec{e}_p^{\,u}\,,\ p\in\Omega\}$ and $\{\vec{e}_p^{\,s}\,,\ p\in\Omega\}$ constitute a *hyperbolic structure* on Ω. The directions $\vec{e}_p^{\,s}$ and $\vec{e}_p^{\,u}$ are called, respectively, the *stable* and the *unstable* directions at a point p.

Note that equivalent metrics in (1.2) give the same value of the Lyapunov exponent. Since in the case of compact S all Riemannian metrics are equivalent, the Lyapunov exponents are independent of the choice of the metrics. Of course, they do depend in the case of noncompact S. Note that the existence everywhere of the limits in (1.2) is proven by Oseledets [O].

Our conjecture follows from Pesin's theory, if we prove that the chaotic zone has positive Lebesgue measure and possesses a hyperbolic structure. At least, this is exactly what Pesin asserts in [Pes2].

So, the main question can be formulated as *how to find a hyperbolic structure?* In [L1] the second author started an attempt to prove the existence of a hyperbolic structure for the standard map at least for large values of the parameter of the map. The work is still in progress and not yet finished, but, as a by–product, after producing a lot of numerical simulations, we obtained an unexpected method which enables an observer to *see* this hyperbolic structure in the phase space of the system by using a computer as a microscope. The method is based on some features of systems with coexistence of regular and chaotic behaviour, and has no analogue in the case of the so called Anosov systems, i.e., systems with pure chaotic motion. Roughly speaking, the visualisation method is based on the fact that *the traces of regular motions mark the boundaries of (pseudo–)parallelogramms of a Markovian pseudo–partition of an intrinsic hyperbolic structure.*

§2. Description of a model. A shrinking property.

Before describing the visualisation method, let us dwell on the description of the model which we used and its properties. Following Carleson [Ca] we will consider a self–map F of the 2–torus $\mathbb{T}^2 = \mathbb{R}^2/\mathbb{Z}^2$ defined by the formula

$$
F : \begin{pmatrix} x \\ y \end{pmatrix} \longmapsto \begin{pmatrix} gf(x) - y \\ x \end{pmatrix}\,. \tag{2.1}
$$

Here f is a smooth real valued periodic function with period 1, having a finite number of critical points on the period, all of them are supposed to be nondegenerated and g is a large parameter. This map preserves the area. It can serve as a good model to study stochastic phenomena in conservative dynamics [Ch],[Ca]. We note that for $g = 0$ the map is a rotation by $\pi/2$. Let h be a primitive function of f. If g is small then F^4 is close to the time g flow of the Hamiltonian $H(x, y) = h(x) + h(-x) + h(y) + h(-y)$. Of course, if f is even, as we shall consider in our case, the terms of order g in the expression of $F^4 - Id$ cancel and one has to proceed to second order. Then, if f is even, F^4 is close the the time g^2 flow of the Hamiltonian $H(x, y) = f(x)f(y)$. For some properties of this map, in a different context, we refer to §3.4 in [BST]. In particular, it seems that for any value of g the map do not possesses *rotational invariant curves*, i.e., invariant curves which are not contractible to a point in the torus, in contrast with what happens for the Chirikov standard map.

The map (1.1) is a particular case of (2.1) with $f(x) = \cos 2\pi x$ and $g = 0.2$. As one can see from Fig.1, this map can display a chaotic motion. As numerical simulations show, the portion with chaotic motion grows if the parameter g grows (see Fig.11e, for instance). For large values of the parameter the chaotic component occupies, visibly, almost all phase space except, probably, some small islands (see [ST1]). One can try to consider large values of g, and create a kind of “asymptotic” theory of chaos. The hyperbolicity, which is responsible for the presence of the chaotic motion, according to Pesin, is produced by the tangent map, the matrix of which at a point $p = (x, y)$ reads:

$$F'(p) = \begin{pmatrix} gf'(x) & -1 \\ 1 & 0 \end{pmatrix} . \tag{2.2}$$

The matrix (2.2) can be factored in the product of the matrix of a linear hyperbolic map and two rotation matrices with the same angle α:

$$\begin{pmatrix} gf'(x) & -1 \\ 1 & 0 \end{pmatrix} = R(\alpha) \begin{pmatrix} \lambda & 0 \\ 0 & \lambda^{-1} \end{pmatrix} R(\alpha) , \tag{2.3}$$

where $\lambda - \lambda^{-1} = gf'(x)$, and $\tan\alpha = \lambda^{-1}$.

If the x coordinate of a point p is not close to a critical point of f, then, assuming the parameter g to be large, one can deduce that $F'(p)$ is close to a diagonal hyperbolic matrix with a large number λ at the first place of the diagonal, and with λ^{-1} at the second place. One can see that the map F manifests good hyperbolic features everywhere in the phase space, except in narrow strips where x is close to a critical point of f (see Fig.2).

Our method consists in studying the images, $\xi_n = F^n\xi_0$, under iteration by F of a smooth foliation ξ_0. We take as ξ_0 the foliation by *horizontal* lines, $y = const$. The first observation is that, after the first iterate, the foliation acquires *folds*. These are the points where ξ_1 is *vertical*. A *line of folds* for ξ_1 (or, in general, for ξ_n) is the locus of the points where ξ_1 is vertical. Each fold corresponds to a critical point of f. To explain this, let us represent the map F, given by (2.1), as a superposition of two maps: $F = F_2 \circ F_1$, where

$$F_1 : \begin{pmatrix} x \\ y \end{pmatrix} \longmapsto \begin{pmatrix} x \\ y - gf(x) \end{pmatrix} , \qquad F_2 = R(\pi/2) : \begin{pmatrix} x \\ y \end{pmatrix} \longmapsto \begin{pmatrix} -y \\ x \end{pmatrix} . \tag{2.4}$$

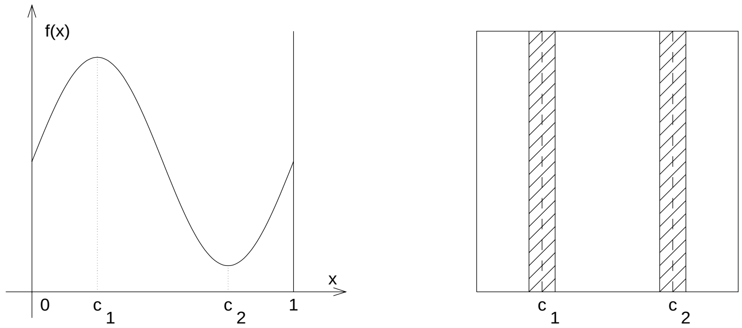

Figure 2. The graph of the function f with two critical points c_1, c_2 . The strips in the phase space with weak hyperbolic properties of the first iterate of the map (2.1) are shown to the right.

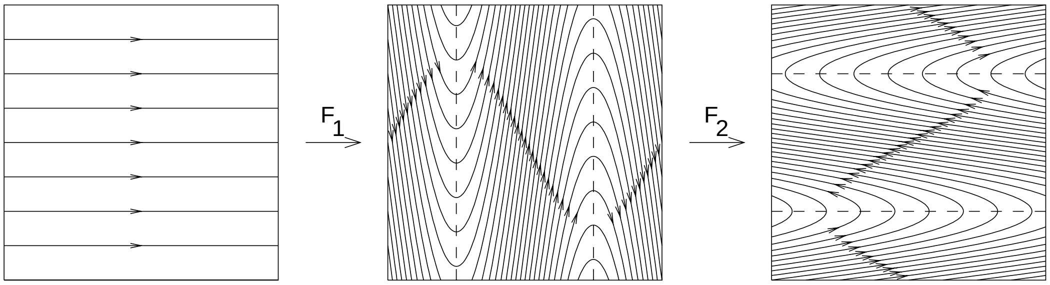

Figure 3. Creation of folds after the first iterate.

The results of subsequent applications of the maps F_1 and F_2 are shown in Fig.3.

The first map, F_1 , is a shear in the vertical direction, while the second map, F_2, turns the result by $\pi/2$. Note that, in the case of big g, the tangent direction (in the projective sense) of ξ_1 is close to the one of ξ_0 except at narrow horizontal strips which are the images of the critical vertical strips of Fig.2.

What happens with the folds if we subject them to further iterates? Each fold shrinks, and the shrinking can be decomposed into two operations of a different nature:

(1) *Dynamical shrinking.* This means that any square box, containing a fold, becomes a rectangular one after applying a linear map with diagonal matrix of the form $\begin{pmatrix} \lambda & 0 \\ 0 & \lambda^{-1} \end{pmatrix}$ (recall that, if we are far from a critical line, then the representation (2.3) gives us the closeness to a diagonal matrix), and all vertical distances, therefore, are subjected to a shrinking with factor λ^{-1} .
(2) *Geometrical shrinking.* Every angle, after applying the diagonal linear map, shrinks by a factor λ^{-2} (see Fig.4). If we control the image by measuring the angle which the lines create with the horizontal direction, we should diminish the size of the strip by the said factor λ^{-2} in order to observe inside the strip the same size of the deviation from the horizontal direction.

The total shrinking factor for the curvatures, which takes into account both

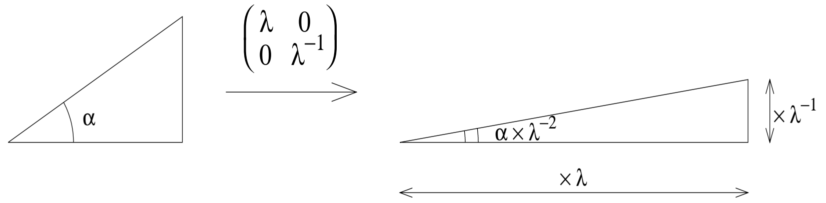

Figure 4. Shrinking of an angle by the factor λ^{-2}.

mechanisms, is λ^{-3}. This will be illustrated later on, in figures 8 and 9.

The idea of the proof of the existence of a hyperbolic structure is to perform all the iterates, exclude all "bad" strips, and try to get convergence of the tangent directions, in the projective sense, to the unstable directions ($n \to +\infty$) on the complement of the bad strips. This should be of big measure if g is big.

§3. The visualisation method.

We were astonished when we discovered that one could immediately see the "bricks" of a (hypothetic) hyperbolic structure by just applying the following simple procedure. Let us consider, for the sake of the symmetry, the sequences of iterates of the initial foliation ξ_0 in both directions:

$$\xi_n = F^n \xi_0\,, \quad \xi_{-n-1} = F^{-n-1}\xi_0\,.$$

We take the $(-n-1)$–th iterate because ξ_{-n-1} is symmetric with respect to ξ_n via the symmetry (in fact a reversor) $S\colon (x,y) \to (y,x)$.

Denote by $\vec{e}^{\,u}_n(p)$ the tangent vector to ξ_n at a point p. More precisely,

$$\vec{e}^{\,u}_n(p) = \begin{pmatrix} e^{\,u}_{n,1}(p) \\ e^{\,u}_{n,2}(p)\end{pmatrix} = \frac{\vec{X}_n(p)}{\|\vec{X}_n(p)\|}\,, \tag{3.1}$$

where

$$\vec{X}_n(p) = (F^n)'\,(p_{-n})\vec{X}_0\,, \qquad \vec{X}_0 = \begin{pmatrix}1\\0\end{pmatrix}, \tag{3.2}$$

with $p_{-n} = F^{-n}(p)$, and we use the euclidean norm in $\mathbb{R}^2$. Analogously, let $\vec{e}^{\,s}_n(p)$ denote the unit tangent vector to ξ_{-n-1}, that is,

$$\vec{e}^{\,s}_n(p) = \begin{pmatrix} e^{\,s}_{n,1}(p) \\ e^{\,s}_{n,2}(p)\end{pmatrix} = \frac{\vec{X}_{-n-1}(p)}{\|\vec{X}_{-n-1}(p)\|}\,, \tag{3.3}$$

where

$$\vec{X}_{-n-1}(p) = \left(F^{-n}\right)'(p_n)\vec{X}_{-1}\,, \qquad \vec{X}_{-1} = \begin{pmatrix}0\\-1\end{pmatrix}, \tag{3.4}$$

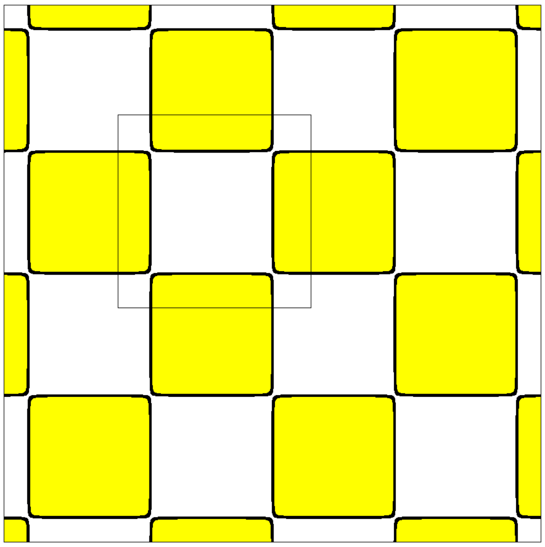

Figure 5. Plot corresponding to $g = 3.1$, 1 iterate, window $[-1.1, 1.1] \times [-1.1, 1.1]$ and $\delta = 0.5$. The domain of Fig.6a is displayed.

with $p_n = F^n(p)$.

Consider the sinus of the angle, $\alpha_n(p)$, between $\vec{e}_n^{\,u}(p)$ and $\vec{e}_n^{\,s}(p)$:

$$\sin \alpha_n(p) = \begin{vmatrix} e^u_{n,1}(p) & e^s_{n,1}(p) \\ e^u_{n,2}(p) & e^s_{n,2}(p) \end{vmatrix} . \tag{3.5}$$

It appears that the *level lines* of the function (3.5) display some structure in chaotic regions which can be apparently interpreted as a hyperbolic one.

We have done several experiments with the model (2.1) taking $f(x) = \cos 2\pi x$ and with different values of the parameter g. The procedure we used can be called a *renormalization procedure.* We understand the renormalization in the following sense:

$$\boxed{\textit{Renormalization} = \textit{Zoom} + \textit{An increase of the number of iterates}}$$

In the forthcoming figures we use the following code of colours: black for p such that $|\sin \alpha_n(p)| < \delta$, grey if $\sin \alpha_n(p) > \delta$ and white if $\sin \alpha_n(p) < -\delta$. Here δ is some cutting value.

§4. The first sequence of renormalizations. The case of big g.

Our first sequence of pictures corresponds to model (2.1) with $f(x) = \cos 2\pi x$ and $g = 3.1$, which should be considered as a big value, because the corresponding value of the expanding factor, λ, can be evaluated through its maximum value $\lambda = 2\pi g \approx 19.48$. The first picture of this sequence shows a part of the plane $\mathbb{R}^2$ defined by the inequalities $-1.1 \le x \le 1.1$, $-1.1 \le y \le 1.1$, which represents the unfolding of the torus (see Fig.5). The number of iterates is $n = 1$. We take here, and for all subsequent figures of this sequence, the cutting value $\delta = 0.5$.

The following series shows three subsequent steps of the renormalization process. We start with a magnification (Fig.6a) of the square shown in Fig.5, increase the

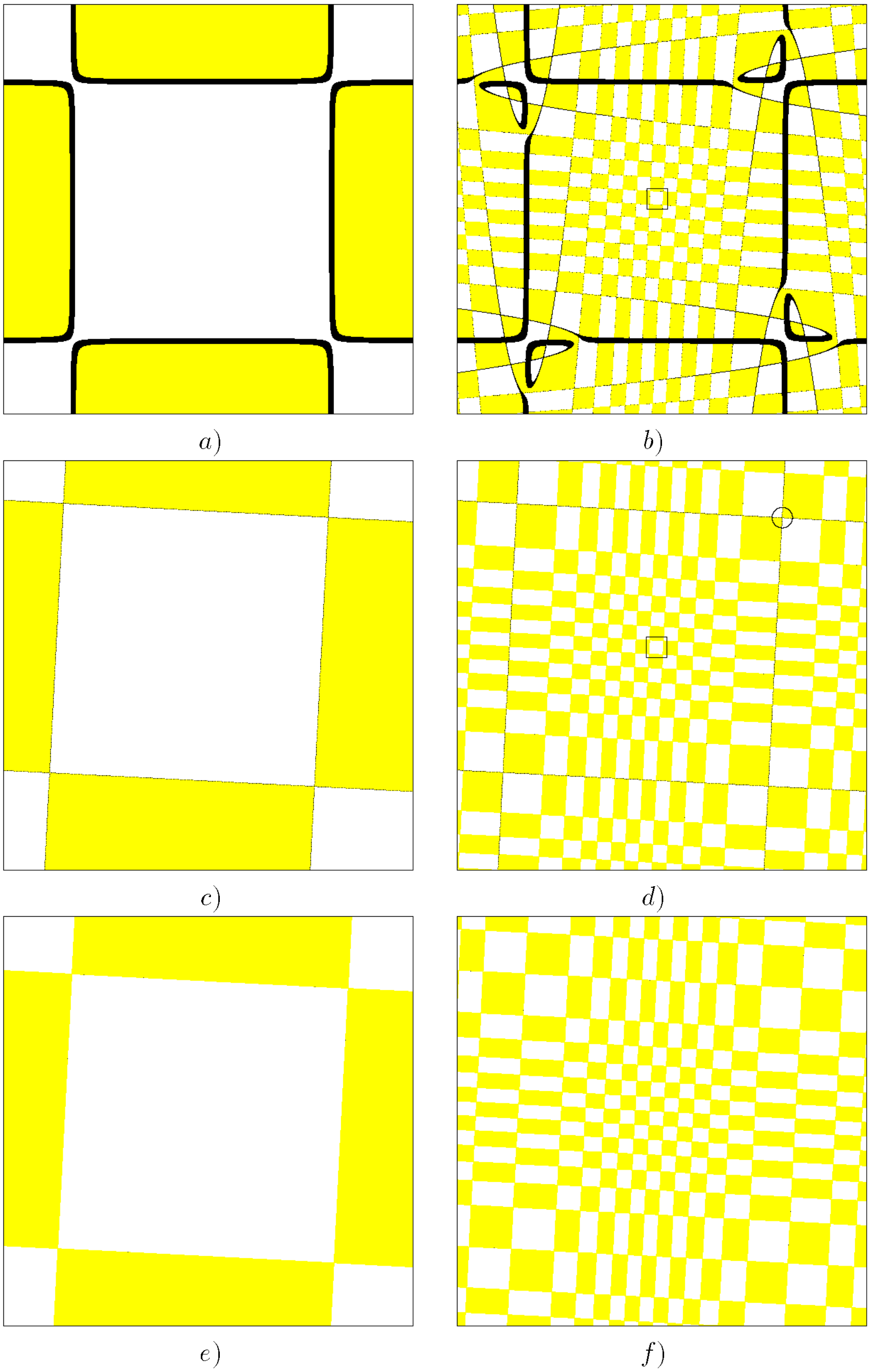

Figure 6. Plots corresponding to $g = 3.1$, $\delta = 0.5$. The respective windows and numbers of iterates are as follows: $a)$ $[-0.2383 \pm 3.955 \times 10^{-1}] \times [0.2540 \pm 3.955 \times 10^{-1}]$, $n = 1$. $b)$ window as in $a)$, $n = 2$. $c)$ $[-0.24681 \pm 1.977 \times 10^{-2}] \times [0.27382 \pm 1.977 \times 10^{-2}]$, $n = 2$. $d)$ window as in $c)$, $n = 3$. $e)$ $[-0.24732\,6 \pm 9.89 \times 10^{-4}] \times [0.27556\,3 \pm 9.89 \times 10^{-4}]$, $n = 3$. $f)$ window as in $e)$, $n = 4$. The windows in $c)$ and $e)$ are magnifications of the regions marked with a small square in $b)$ and $d)$, respectively. An area around the center of the circle in $d)$ is shown in Fig.7a.

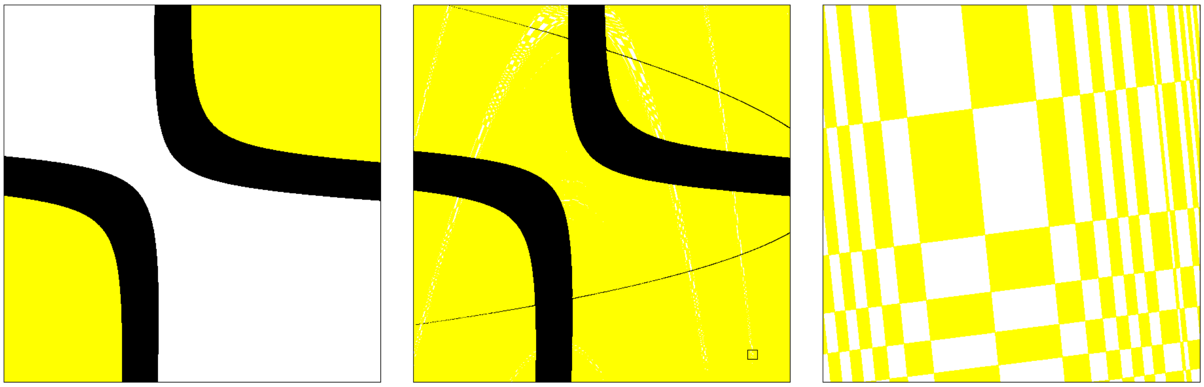

a) *b*) *c*)

Figure 7. Plots corresponding to $g = 3.1$, $\delta = 0.5$. The respective windows and numbers of iterates are as follows: *a*) $[-0.23518\ 286 \pm 7.06 \times 10^{-6}] \times [0.28809\ 545 \pm 7.06 \times 10^{-6}]$, $n = 3$. *b*) window as in *a*), $n = 12$. *c*) $[-0.23517\ 71968 \pm 1.513 \times 10^{-7}] \times [0.28808\ 94148 \pm 1.513 \times 10^{-7}]$, $n = 12$. The magnification in *c*) corresponds to the domain marked in *b*) near the right lower corner.

number of iterates ($n = 2$, Fig.6b), choose a smaller square in Fig.6b, magnify it (Fig.6c), increase the iterates ($n = 3$, Fig.6d), again choose a window in Fig.6d, magnify it (Fig.6e) and increase the iterates ($n = 4$, Fig.6f).

Comparing Fig.6d and Fig.6f one can observe a great similarity, as it also happens between Fig.6c and Fig.6e . Both pictures contain, essentially, only two colours. The black colour is almost invisible in both pictures because the black strips are extremely thin. Recall that the width of the black strip, according to the shrinking property, described in §2, decreases at each iterate by the factor λ^{-3} whilst the size of a *cell* decreases by the factor λ^{-1}. The picture looks like a (nonuniform) chess–board, but the corners are not really the intersections of the boundary line. In a microscopic scale one can observe the same *quasi–intersection* as in Fig.5. This is illustrated in Fig.7a: the corner, marked in Fig.6d as the center of a circle, is magnified, the width of the window being now close to 1.4×10^{-5}.

Fig.7b shows the same as Fig.7a, but with 12 iterates (while Fig.7a uses 3 iterates). A magnification of a small square in Fig.7b is shown in Fig.7c. One can see how the area in the quasi–intersection is filled by “hyperbolic bricks”.

We must recall here the meaning of the colours in the pictures. They show the sign of the determinant (3.5). The chess–board structure, the cells of which become smaller and smaller by the increase of the number of iterates, shows that the vectors of the basis $\{\vec{e}_n^{\,s}(p), \vec{e}_n^{\,u}(p)\}$ turn very quickly when the point p crosses the chess–board area. Also, this frame turns by π when p passes a *strait* of a quasi–intersection (see Fig.8).

Note also that the sizes of a cell of the *quasi–partition* of Fig.8 are of the order $e^{-n\chi}$ because the opposite sides originate from different critical values of the function f. For example, the sides which are parallel to $\vec{e}_n^{\,s}$ go to the vertical strips on Fig.2 after applying F^n. The directions of the sides of a cell are close to the stable and unstable directions in the middle of the cell. As said in §2, a scaling by λ^{-1} in the size of the *cells* of the *quasi–partition*, corresponds to a scaling by λ^{-3} in the curvatures at the *corners* and in the size of the *straits* (see again Fig.8).

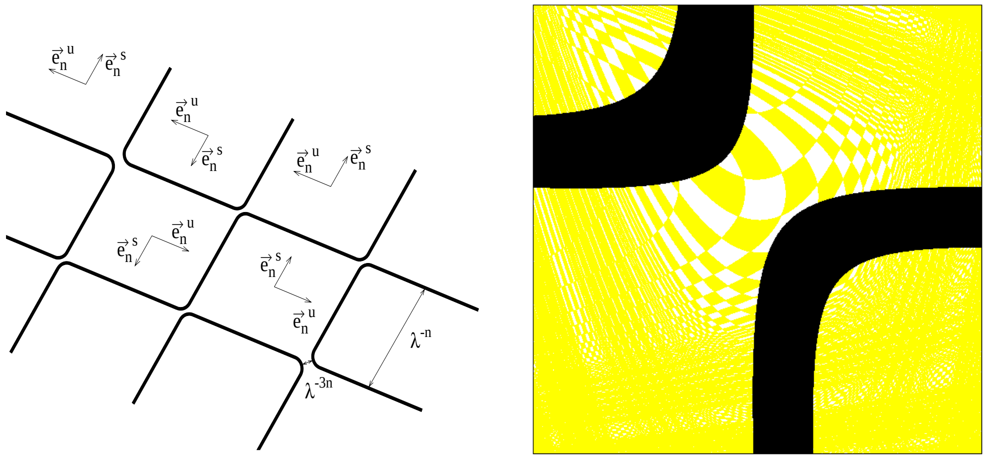

Figure 8. Left: A quasi–partition by zero lines of $\sin \alpha_n$. Positions of the frame defined by $\{\vec{e}_n^{\,s}(p), \vec{e}_n^{\,u}(p)\}$ in different places of the web. Right: An illustration of the turns of the frame at the strait using $g = 2.2$, $n = 11$, $\delta = 0.5$ and the window $[0.23071\,7, 083 \pm 1.872 \times 10^{-5}] \times [0.26928\;602 \pm 1.872 \times 10^{-5}]$.

§5. Irregularities and islands.

The preceding experiment may give an illusion that the hyperbolic structure inside a chaotic area is quite simple and regular. But this impression is wrong. Sporadic irregularities can happen. The origin of these irregularities can be described as follows. When one passes from the n–iterate to the $(n+1)$ one, the lines of folds of the new generation, i.e., of the $(n+1)$–th iterate, create a more tiny web than those of the n–iterate. Fig.9 shows the effect of F on a quasi–intersection of two lines of folds. For this illustration $g = 2.1$ has been taken. In Fig.9a we have plotted different level lines of the argument of ξ_2, the image for $n = 2$ of the initial foliation ξ_0 . In particular two lines of folds, corresponding to an argument of $\pi/2$, are marked by arrows. Similar lines for ξ_3 are shown in Fig.9b, but they are much more compressed in the vertical direction and expanded in the horizontal one (in both cases by a factor λ.) For completeness, the images under F of the lines of Fig.9a are displayed in Fig.9c, with the same window as in Fig.9b. Due to (2.2) the lines of argument $\pi/2$ in Fig.9a become lines of zero argument in Fig.9c. In fact Fig.9 gives information on the argument of $\vec{X}_n(p)$, as defined by (3.2), rather than just on the argument of ξ_n .

Figure 9 shows also how the action of the map resolves in some sense the complicated unstable configuration into simple stable elements. Among them one can find the so called *cusp* singularity, where two lines of folds meet. The cusp singularity (see Fig.10) is stable, i.e., it is not destroyed by successive iterations. A local model of the foliation near a cusp is given by the integral lines of the vector field $\left(\xi + \frac{1}{2}\eta^2\right) \frac{\partial}{\partial \xi} + \frac{\partial}{\partial \eta}$.

It is an experimental fact that two cusps, one of ξ_n , another of ξ_{-n-1} , can produce an island when they meet. We illustrate this phenomenon with the same model (2.1) where $f(x) = \cos 2\pi x$, and $g = 2.1602$. The value of the parameter g has been adjusted so that such a meeting occurs. The point in the center of the island remains elliptic (or some point bifurcating from it remains) for g between 2.16014 and 2.16083, roughly.

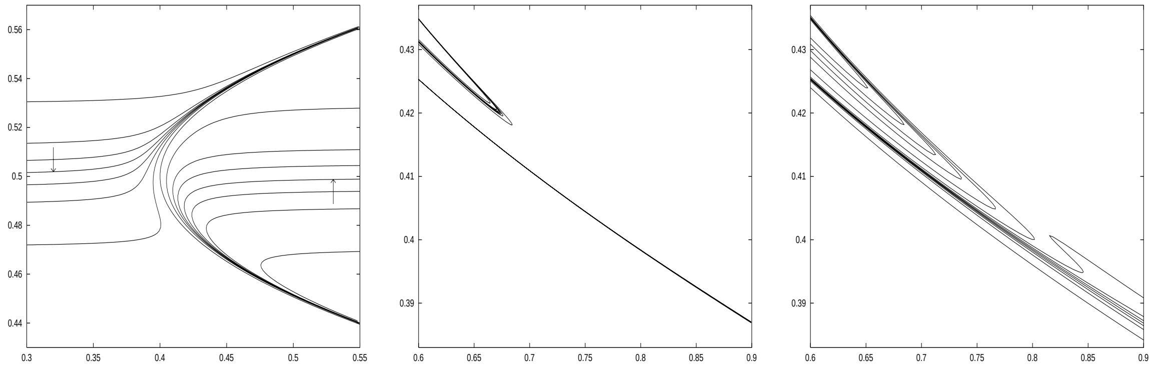

a) *b)* *c)*

Figure 9. A quasi–intersection of two lines of folds and the effect of F. *a)* Lines of constant argument of ξ_n are shown for $n = 2$ and $g = 2.1$. The arguments of $\vec{X}_2(p)$, in multiples of $\pi/8$, for the different lines drawn (labelled by the point of intersection with the right part of the frame, from top to bottom) are: 1, 2, 3, 4 (fold line), 5, 6, 7, 8 (equivalent to -8), -7, -6, -5, -4 (fold line), -3, -2, -1 and then, again, -1, -2, -3, -4, -5, -6, -7, -8. *b)* Similar for $n = 3$ located near the image under F of the *a)* case. The arguments of $\vec{X}_3(p)$, in multiples of $\pi/8$, for the different lines drawn (labelled by the point of intersection with the left part of the frame, from bottom to top) go from -8 to -1, then from 0 to 7 and, again, from 7 to 0. *c)* Images under F of the lines of *a)* using the window of *b)*. The displayed lines correspond to the ones of *a)* turned almost by π. The lines of label -2 and -1 fall outside the window.

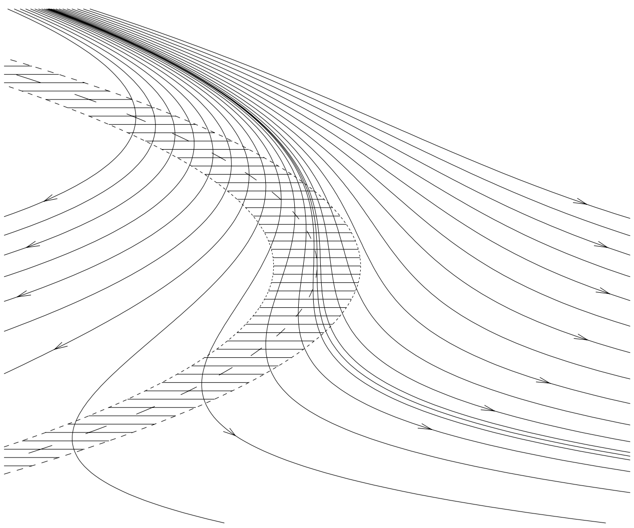

Figure 10. The geometry near a cusp. Two fold lines (drawn in broken lines and making, together, a kind of parabola) meet. The shaded area corresponds to the points with the argument of $\vec{X}_n(p)$ close to $\pi/2$.

One can see in Fig.11a the meeting of two cusps in a small window. $\delta = 0.25$ has been used in all parts of Fig.11. The number of iterates is $n = 7$. The second picture represents the same area, but with $n = 30$. An island is visible, surrounded by the sea of chaos. It is easy to check that the island has period 8 and the central point has $x = y = a \simeq 0.85955\ 91975$. The value a satisfies the following condition:

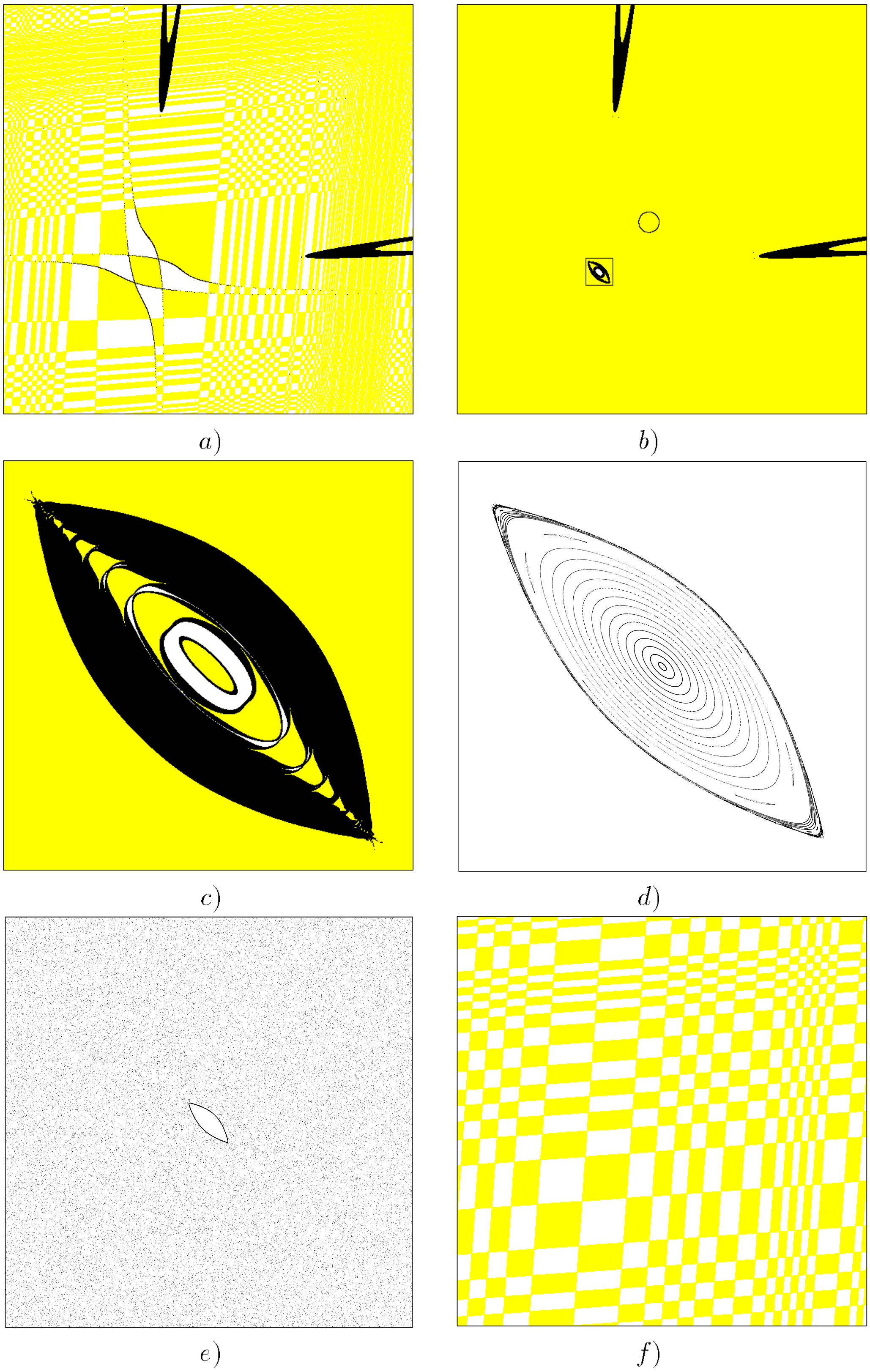

Figure 11. Meeting of two cusps and island for $g = 2.1602$: $a)$ $n = 7$, window $[0.86011\,5 \pm 1.811 \times 10^{-3}] \times [0.86003\,6 \pm 1.811 \times 10^{-3}]$. $b)$ window as in $a)$, but $n = 30$, showing the appearition of an island. The square inside corresponds to picture $c)$ and picture $f)$ is located around the center of the marked circle. $c)$ Magnification of $b)$ with $n = 240$ and central point (of period 8) with $x = y = 0.85955\,91975$. Width 2.4×10^{-4}. $d)$ same as $c)$ but showing orbits in the island. $e)$ Iterates of $x = y = 0.85959\,11975$, slightly outside the island, falling in the window of width 2×10^{-3} around the periodic point. A total of 2.5×10^{11} iterates has been used. An approximate "last" invariant curve, with initial point $x = y = 0.85959\,08098$, is also drawn. $f)$ The chess–board structure with $n = 20$, window centered at $x = y = 0.86$ and width 10^{-12}.

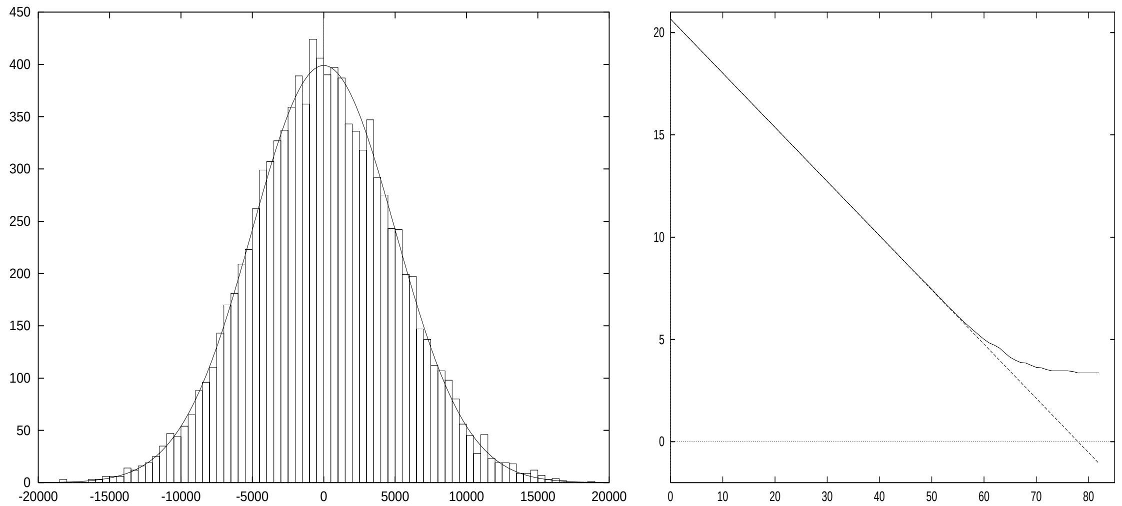

Figure 12. Left: Histogram of the errors with respect to the equipartition for the simulation mentioned in the text. The corresponding (scaled) density function of the normal law with the theoretical variance has been also plotted. Right: Logarithm of the experimental (continuous line) and theoretical (broken line) number of "empty" boxes from a total of 30720×30720 boxes, as a function of the number of blocks of 2.5×10^8 iterates. See the text for additional explanation.

Let (a, a) be an initial point, and (b, a) and (c, b) the first and second iterates, respectively. Then one must have $b + c = 1/2 \pmod 1$. The symmetries of f in our case ($f(-x) = f(x)$, $f(x + 1/2) = -f(x)$) imply that (a, a) has period 8, the periodic orbit being symmetric with respect to the diagonal, $x = y$, and also with respect to the point $(1/4, 1/4)$. Furthermore (a', a'), with $a' = b - 1/2$ (mod 1), gives also rise to a symmetric 8–periodic orbit with the same eigenvalues. It will be named the "companion orbit" of the first one. From the points of the first orbit, $\{(x_j, y_j),\ j = 1, \ldots, 8\}$, one obtains the points of the companion orbit $\{(u_j, v_j),\ j = 1, \ldots, 8\}$, by $u_j = -x_j$, $v_j = y_j - 1/2$, but they are mapped by F in a different order. In Fig.11c we show a magnification of the previous picture. The number of iterates has been increased up to 240. The zones of different colour around the elliptic periodic point show the variation of the rotation number (it decreases) when we go away from the periodic point towards the boundary of the island. The "last" invariant curve has a small rotation number (strictly less than 1/9), and there are two nearby hyperbolic periodic points of period 8. Suitable branches of the separatrices of these points are close to the "last" invariant curve (see [ST2] for practical methods to approximate this curve).

Fig.11d displays some orbits around the periodic elliptic point. The orbit of a point slightly outside the island (shifted in x and y by 3.2×10^{-5} with respect to the periodic point), generates a chaotic sea which seems to cover almost all of the phase space, i.e., the full torus. More concretely, if in the full window, $[0, 1] \times [0, 1]$, a grid of 4500×4500 pixels is used, all of them contain points of the orbit after 4×10^8 iterates (this can depend on the arithmetics). This evidences that no islands of width much more large than the one displayed in Fig.11 exists for the present value of g (see later the description of a final test). A longer simulation, starting at the same point and using $n = 2.5 \times 10^{11}$ iterates, has been done. Fig.11e displays a part of this orbit on a window around the periodic point. For comparison, an approximate last invariant curve, with initial point also on the diagonal, is also drawn. The arithmetic errors play a significant role, but *the iterates should not enter inside islands.* Fig.11e shows the iterates falling in the window $[a \pm 10^{-3}] \times [a \pm 10^{-3}]$, where a was given before. In principle, and disregarding the presence of the island, 10^6 iterates must fall in the window if exact equipartition occurs. In the simulation we carried out this number was 997171, showing a remarkable agreement. (Again, this depends on the arithmetics, operating system, compiler and program). As an additional test, the full phase space was divided in 100×100 square boxes of the form $[i/100, (i+1)/100] \times [j/100, (j+1)/100]$, $i, j = 0, \dots, 99$. The number of iterates falling in each box was recorded. Equipartition would imply an average value of 2.5×10^7 iterates per box. The largest deviations observed, among the 10^4 boxes, were -22949 and $+18762$. Again a very good agreement with an assumption of ergodicity with respect to the Lebesgue measure in the chaotic sea. Fig. 12 (left) shows the histogram of the distribution of the errors with respect to the average value. Each interval in the figure has a width of 500 units. As vertical variable the number of boxes for which the error falls in this interval has been plotted (without dividing this value by 500). It is close to the theoretical value, which is approximated by $10^4 \times 500$ times a normal law with zero mean value and standard deviation $[2.5 \times 10^{11} \times 10^{-4} \times (1 - 10^{-4})]^{1/2}$.

A final test, during this simulation, was the following: Consider the full window divided in $B = 30720 \times 30720$ equal square boxes, similar to the 100×100 grid above. When an iterate falls in one box, the box is marked as "full". After every block of 2.5×10^8 iterates, the *experimental* number of "empty" boxes, E_E, was recorded. According to Poisson law, the *theoretical* number of empty boxes after N iterates is given by $E_T = B \exp(-N/B)$. Fig.12 shows, on the right, the logarithms of both the experimental and theoretical values, E_E and E_T, as a function of the number of block iterates. A perfect agreement is seen for the initial blocks. At the end, the experimental value stabilizes to 29 boxes. They correspond to the ones inside islands. Only the period 8 islands described before and the "companion islands" have been detected. Even not all the 16 islands can be "seen" by looking at the empty boxes, because some of them are extremely narrow (beyond 10^{-5}) and only 4 have been seen.

To be sure that the chaotic sea bears the same kind of hyperbolic structure as we have seen in §4, in Fig.11f we have enlarged a small square, located in Fig.11b around the center of the circle marked on it. We have taken $n = 20$ and a quite small width (10^{-12}). At each increase of n corresponds a suitable reduction of the size of the window. In Fig.11f the central point is also on the diagonal, but a similar behaviour is obtained also for arbitrary points (see next section).

§6. The case of small values of g.

There might be an impression that all the effects we are studying are due to the strong hyperbolicity of the matrix (2.3) when g is big enough. But there is another big parameter here which occurs in all dynamics generated by area preserving maps, namely the number of iterates, n. Even if g is small, one can see chaotic zones. We

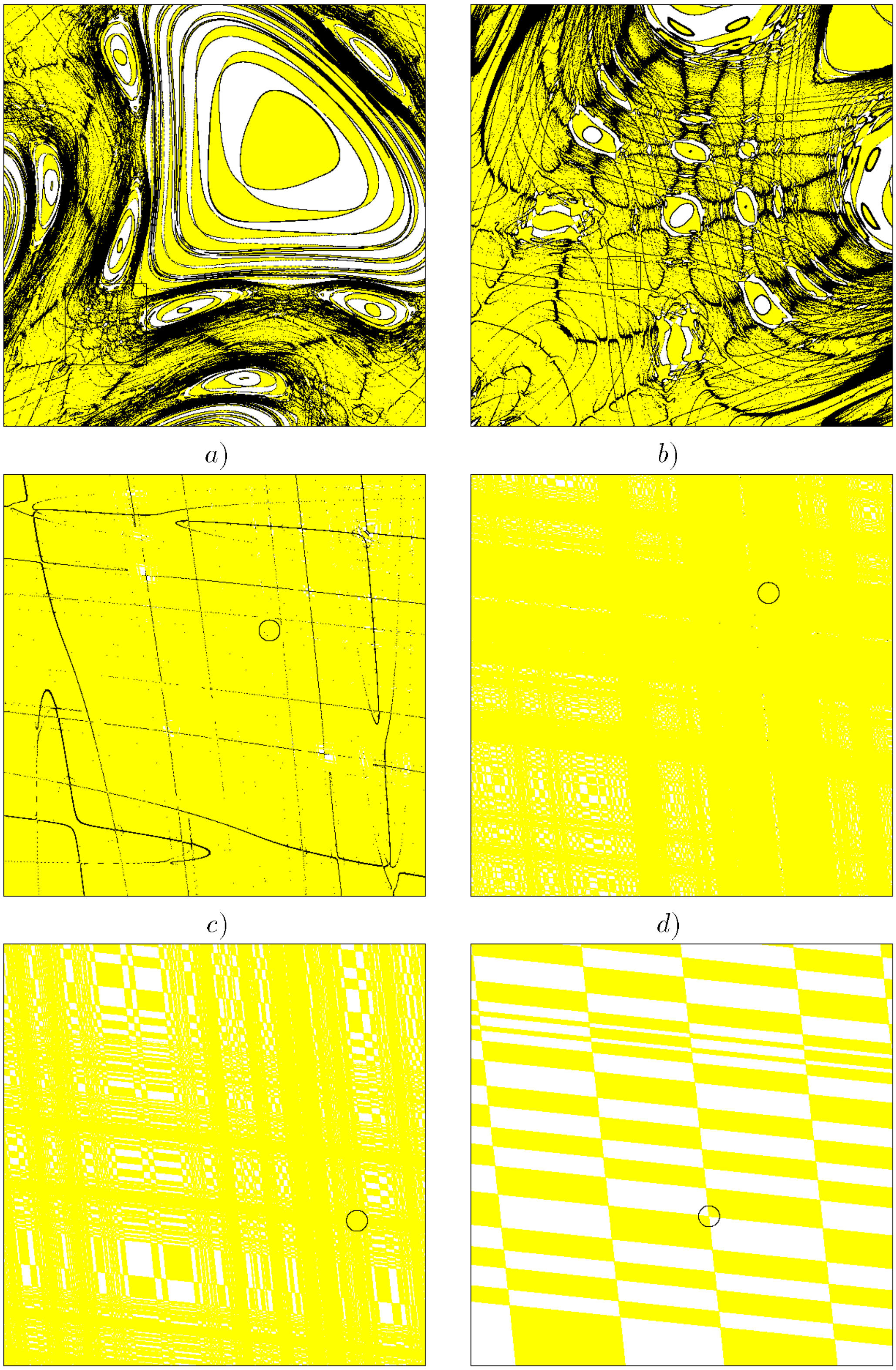

a) b) c) d) e) f)

Figure 13. A sequence of magnifications for $g = 0.2,\ n = 250$. $\delta = 0.02$ for the initial plot, $\delta = 0.05$ for all the others. Windows: $a)$ $[\pm 0.25] \times [\pm 0.25]$.
$b)$ $[-0.1292 \pm 4.82 \times 10^{-2}] \times [-0.1292 \pm 4.82 \times 10^{-2}]$.
$c)$ $[-0.14237 \pm 3.79 \times 10^{-3}] \times [-0.14237 \pm 3.79 \times 10^{-3}]$.
$d)$ $[-0.14138\,18 \pm 1.21 \times 10^{-5}] \times [-0.14138\,09 \pm 1.21 \times 10^{-5}]$.
$e)$ $[-0.14137\,68120 \pm 7.23 \times 10^{-8}] \times [-0.14137\,55976 \pm 7.23 \times 10^{-8}]$.
$f)$ $[-0.14137\,67631\,17 \pm 1.66 \times 10^{-10}] \times [-0.14137\,56202\,16 \pm 1.66 \times 10^{-10}]$.
Each picture is a magnification of the square drawn (or of a small square around the center of the circle marked) on the preceding one. See Fig.14 for the meaning of the circle marked on $f)$.

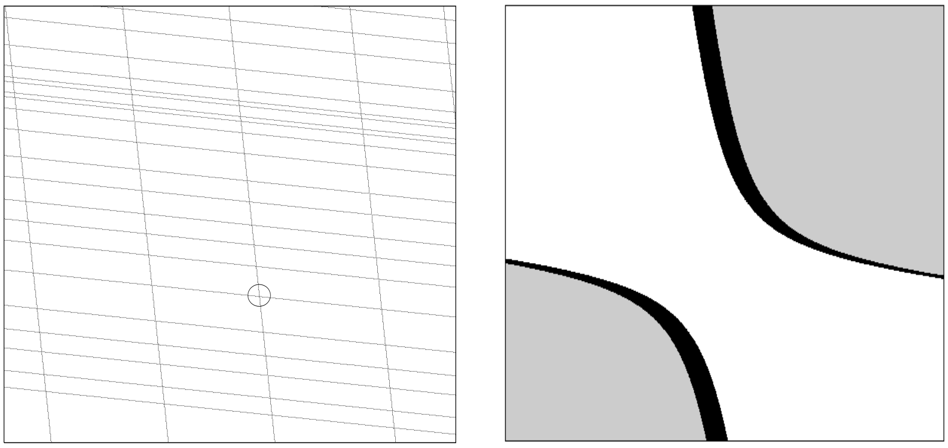

Figure 14. Left: The *quasi–partition* by zero level lines of $\sin \alpha_{250}$ corresponding to the same data and window as in Fig.13f. The lines seem to be perfectly straight but, in fact, they do not intersect, creating *quasi–intersections* instead. Right: A very strong magnification of Fig.13f around the center of the circle marked on it (and also marked on the left part of the present figure). Window: $[-0.14137\ 67630\ 95468\ 03432\ 98655\ 98497 \pm 1.179 \times 10^{-27}] \times [-0.14137\ 56202\ 64460\ 29595\ 01317\ 36326 \pm 1.179 \times 10^{-27}]$.

display if Fig.13 a sequence of pictures showing that the same mechanism works also in the case of small g.

We take $g = 0.2$ as in Fig.1. To show the hyperbolic structure one should take a rather big number of iterates. Our strategy here is a little bit different from that we used before. We fix from the very beginning $n = 250$, a large number, and then proceed to do a sequence of zooms. The first picture, Fig.13a, displays the same area as in Fig.1. Fig.13a is drawn with cutting value $\delta = 0.02$, and $\delta = 0.05$ is used for Fig.13b,...,f. Each subsequent picture is a magnification of the square drawn (or of a small square around the center of the circle marked) on the preceding one.

The last picture of this sequence displays clearly the hyperbolic structure. To underline the perfectness of this picture, we present in Fig.14a a line version of this last figure, that is, only the points where $\sin \alpha_n(p) = 0$ are shown.

The lines look perfectly straight, but in fact they do not intersect, creating quasi–intersections instead. The size of this last window is $d = 3.32 \times 10^{-10}$ and, hence, a typical size of a cell in this domain is of the order of 10^{-10}. One can expect for the width of the strait in the quasi–intersection, to be of the order of 10^{-30}, if one takes into account the λ^{-3} shrinking law per one iterate described in §2. Such narrow details are displayed on the right part of Fig.14, where the size of the actual window is 2.358×10^{-27}. Even smaller details can be uncovered by using arbitrary precision arithmetics. This is perfectly feasible, but it increases largely the computing time.

§7. Conclusion.

The above described pictures of a hyperbolic structure in chaotic regions seem to be typical for area preserving maps with the coexistence of regular and chaotic behaviour. A generalization to higher dimensions can be done by use of a smooth lagrangian foliation instead of ξ_0.

The general impression is that the chaos is well organized. The bulk of the chaotic sea can be decomposed into hyperbolic bricks by the use of the described construction. Some irregularities, like cusps and islands happen rarely. The probability to encounter them along the renormalization process goes to zero exponentially as the number of iterates goes to infinity. One can imagine also that the position of the irregularities is subjected to simple laws.

Nevertheless, it is not clear from our analysis if the number of islands is finite or not. Are the islands dense in the phase space? The results of Duarte [D] are in favour of a positive answer to the last question.

Acknowledgments.

The experimental part of the work was made mainly in May and June 1996 when the second author made short visits to the University of Barcelona and the University of Milano. Preliminary experiments were made, previously, during visits of the second author to the Como branch of the University of Milano. The second author thanks both Universities for their hospitality. The first draft version of the paper was written when the second author was a guest at the Observatory of Nice. He thanks Profs. U. Frisch and A. Morbidelli for this opportunity.

The work was partially supported by INTAS grant 93–339ext. The second author has been also partially supported by CRDF grant RM1-227, RFFI grant 97–01–00612 and a grant of the State Higher Educational Committe in Russia. Visits to Como were supported by a CNR–GNFM grant (Italy). The first and last authors have been partially supported by the European Network Grant ERBCHRXCT 940460. Computing facilities are provided by grants PB94–215 (Spain) and 1996S0GR–105 (Catalonia), who also supported visits of the second author. The paper was finished during a stay of the second author in Barcelona, as visiting scientist, supported by grant SAB1995–0605 (Spain).

REFERENCES

[BCGGS] G. BENETTIN, D. CASATI, L. GALGANI, A. GIORGILLI, L. SIRONI, *Apparent fractal dimensions in conservative dynamical systems*, Phys. Lett. A **118** (1986), 325–330.

[BST] H. BROER, C. SIMÓ, J. C. TATJER, *Towards global models near homoclinic tangencies of dissipative diffeomorphisms*, Preprint, 1996.

[Ca] L. CARLESON, *Stochastic models of some dynamical systems*, Unpublished paper.

[Ch] B. V. CHIRIKOV, *A universal instability of many–dimensional oscillator systems*, Physics Reports **52** (1979), 263–279.

[D] P. DUARTE, *Plenty of elliptic islands for the standard family of area preserving maps*, Annales de l'Institut Henri Poincaré, Analyse non linéaire **11, No 4** (1994), 359–409.

[GLS] V. G. GELFREICH, V. F. LAZUTKIN, N. V. SVANIDZE, *A refined formula for the separatrix splitting for the standard map*, Physica D **71** (1994), 82–101.

[H] M. HÉNON, Current Contents **28 No.4** (1988), 18.

[HH] M. HÉNON, C. HEILES, *The applicability of the third integral of motion: some numerical experiments*, Astronomical Journal **69, No.1** (1964), 73–79.

[LS] V. F. LAZUTKIN, C. SIMÓ, *Homoclinic orbits in the complex domain*, International Journal of Bifurcation and Chaos **7** (1997), 253–274.

[L1] V. F. LAZUTKIN, *Positive entropy for the standard map I* (1994), Prépublications 94–47 Université de Paris–Sud Mathématiques Bâtiment 425 91405 ORSAY France.

[L2] V. F. LAZUTKIN, *Jumping Folds Phenomenon in Area–Preserving Maps* (May 1995), PennState, Department of Mathematics, Report No. PM 190.

[O] V. I. OSELEDETS, *A multiplicative ergodic theorem: characteristic Lyapunov exponents of dynamical systems*, Trans. Moskow Math. Soc. **19** (1968), 197–231.

[Pes1] Ya. B. PESIN, *Families of invariant manifolds corresponding the nonzero characteristic exponents*, Izvestiya Akademii Nauk SSSR, ser.mat. **40:6** (1976), 1332–1379.

[Pes2] Ya. B. PESIN, *Lyapunov characteristic exponents and smooth ergodic theory*, Russ. Math. Surveys **32** (1977), 55–114.

[Po] H. POINCARÉ, *Les Méthodes Nouvelles de la Méchanique Céleste,*Vols 1–3, Gauthier–Villars, Paris, 1892, reprinted by Dover, New York (1957).

[ST1] C. SIMÓ, D. TRESCHEV, *Stability islands in the vicinity of separatrices of near–integrable symplectic maps*, Preprint, 1997.

[ST2] C. SIMÓ, D. TRESCHEV, *Evolution of the "last" invariant curve in a family of area preserving maps: The case of the separatrix map*, Preprint, 1997.

[S] J. M. STRELCYN, *The "coexistence problem" for conservative dynamical systems: a review.*, Colloq. Math. **62, No. 2** (1991), 331–345.

[Z] E. ZEHNDER, *Homoclinic points near elliptic fixed points*, Comm. Pure Appl. Math. **26** (1973), 131–182.

[1] Dipartimento di Matematica, Università degli Studi di Milano, via Saldini 50, 20133 Milano, Italy.
E-mail address: antonio@mi.infn.it

[2] Physics Department, St.-Petersburg State University, Ulyanov str. 1, kor.1, Petrodvorets, St.-Petersburg, 198904, Russia.
E-mail address: lazutkin@onti.niif.spb.su

[3] Departament de Matemàtica Aplicada i Anàlisi, Universitat de Barcelona, Gran Via 585, 08007 Barcelona, Spain.
E-mail address: carles@maia.ub.es